Supporting information

High-level information encryption based on optical nanomaterials with multi-mode luminescence and dual-mode reading

Lin Liu[abc], *Shanshan Peng*[ab], *Peng Lin*[ab], *Ruoping Wang*[abc], *Hongyun Zhong*[ab], *Xia Sun*[d], *Song Liang*[ab], *Junpeng Shi*[abce,]* *and Yun Zhang*[abcde,]*

[a]State Key Laboratory of Structural Chemistry, Fujian Institute of Research on the Structure of Matter, Chinese Academy of Sciences, Fuzhou 350002, China

[b]Xiamen Key Laboratory of Rare Earth Photoelectric Functional Materials, Xiamen Institute of Rare Earth Materials, Haixi Institute, Chinese Academy of Sciences, Xiamen 361021, China

[c]University of Chinese Academy of Sciences, Beijing 100049, China

[d]Fujian Science and Technology Innovation Laboratory for Optoelectronic Information of China, Fuzhou 350108, China

[e]Ganjiang Innovation Academy, Chinese Academy of Sciences, Ganzhou 341000, China

E-mail: shijunpeng10@mails.ucas.edu.cn;

E-mail: zhangy@fjirsm.ac.cn

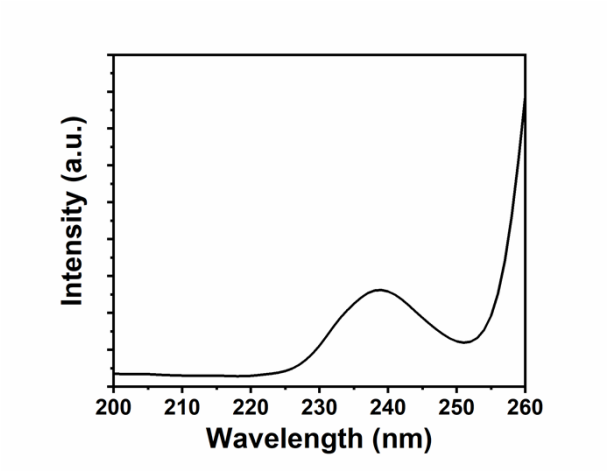

Figure S1. PL excitation spectrum of MLGB monitoring 311 nm emission.

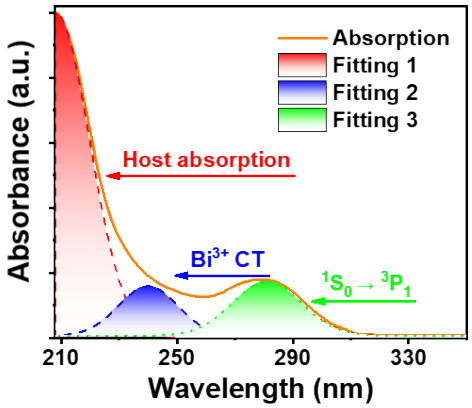

Figure S2. UV-visible absorption spectrum of MLGB with deconvoluted peaks.

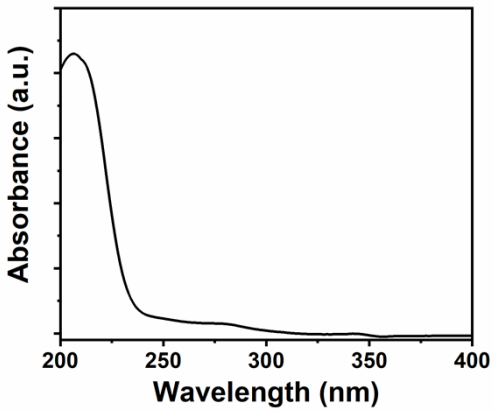

Figure S3. UV-visible absorption spectrum of the host MLG.

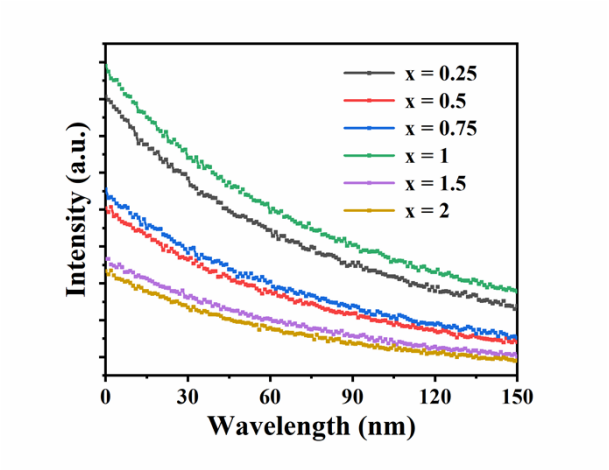

Figure S4. Relationship between the concentration of the dopant Bi^{3+} and the decay of the PersL at 306 nm.

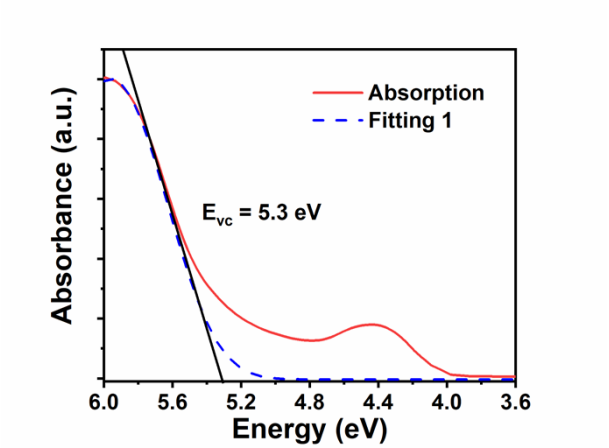

Figure S5. UV-visible absorption spectrum of MLGB and its energy gap.

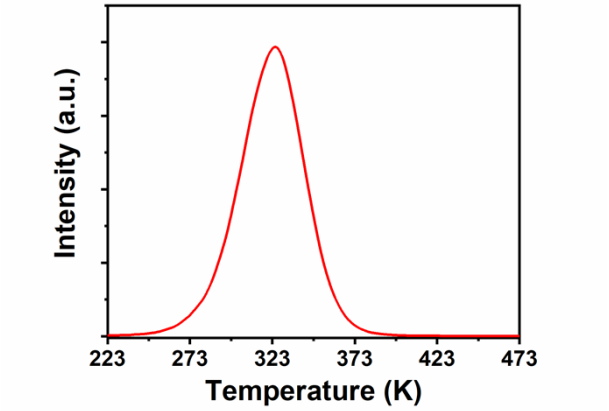

Figure S6. TL spectrum of MLGB.

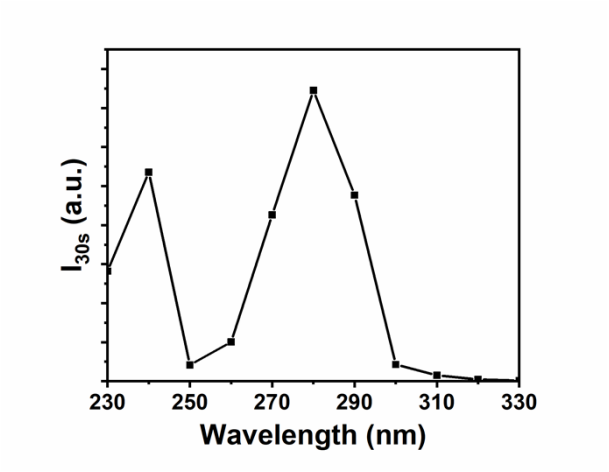

Figure S7. PersL excitation spectrum of MLGB.

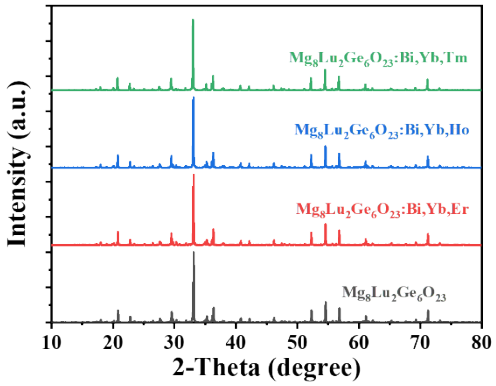

Figure S8. XRD patterns of MLG host and MLGB-Yb/Ln (Ln = Tm, Ho, Er).

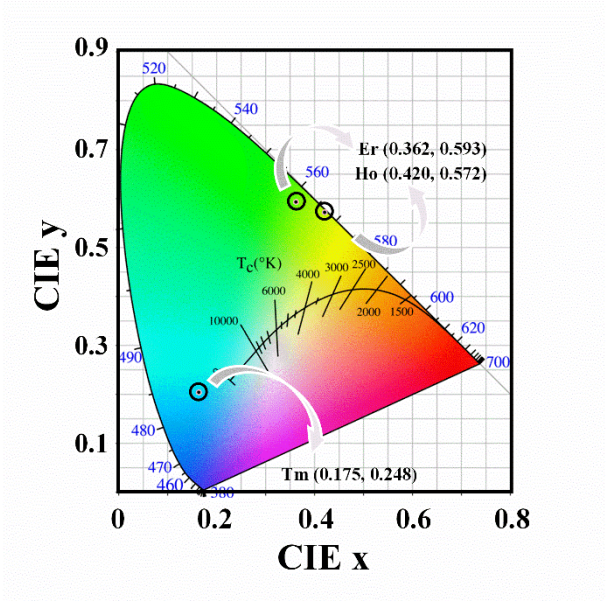

Figure S9. Chromaticity coordinates of MLGB-YB/Ln.

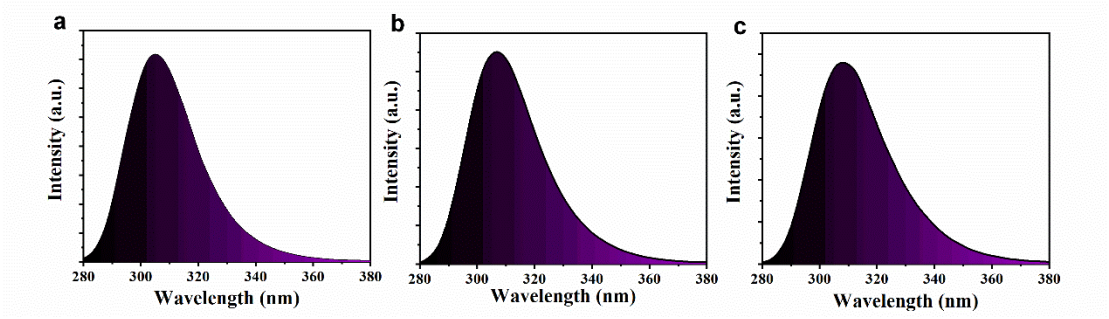

Figure S10. PersL spectra of (a). MLGB-Yb/Tm, (b). MLGB-Yb/Ho and (c) MLGB-Yb/Er.

Table S1. The content of the ions that are really doped into MLG.

Materials/dopants	Bi	Yb	Ln
MLGB	0.590%	-	-
MLGB-Yb/Tm	0.641%	1.362%	0.664%
MLGB-Yb/Ho	0.546%	1.134%	0.640%
MLGB-Yb/Er	0.571%	1.242%	0.574%